ELSEVIER

Polymer 42 (2001) 6801–6810

polymer

www.elsevier.nl/locate/polymer

Effect of temperature and pressure on gas transport in ethyl cellulose membrane

Xin-Gui Li[a,b,*], Ingo Kresse[b], Zhi-Kang Xu[b,c], Jürgen Springer[c]

[a]*Department of Polymer Materials Science and Engineering, College of Materials Science and Engineering, Tongji University, 1239 Siping Road, Shanghai 200092, People's Republic of China*

[b]*Macromolecular Chemistry, Institute of Technical Chemistry, Technical University of Berlin, D-10623 Berlin, Germany*

[c]*Institute of Polymer Science, Zhejiang University, Hangzhou 310027, People's Republic of China*

Received 20 November 2000; accepted 5 February 2001

Abstract

A homogeneous dense ethyl cellulose (EC) membrane has been prepared by a solution casting technique with chloroform as solvent and characterized by wide-angle X-ray diffraction, differential scanning calorimetry, and tensile tester. Permeating characteristics of five pure gases through the membrane has been described in detail. The permeability, diffusivity, solubility, and their selectivities of oxygen, nitrogen, carbon dioxide, methane and hydrogen through the membrane have been measured by a change in operating temperature and upstream pressure in a time-lag apparatus. A continuously enhanced permselectivity for gas pairs of carbon dioxide/methane, and hydrogen/nitrogen, an enhanced diffusivity selectivity for gas pairs of oxygen/nitrogen, carbon dioxide/methane, as well as a decreased permeability and diffusivity for five pure gases, have been observed with decreasing the operating temperature. The solubility of five gases in the EC membrane increases with decreasing temperature. The solubility selectivity does not vary nearly with operating temperature. Especially, the permeability, diffusivity, solubility, and their selectivities in the EC membrane almost maintain constant with changing the upstream pressure. The highest oxygen/nitrogen, carbon dioxide/methane, and hydrogen/nitrogen selectivity coefficients were, respectively, equal to 4.27, 14.7, and 19.5. A relationship between the diffusivity and effective molecule diameter of the gases across the EC membrane was discussed. The gas solubility in the membrane is believed to be a linear function of the critical temperature of the gases. © 2001 Published by Elsevier Science Ltd.

Keywords: Ethyl cellulose membrane; Gas transport; Gas permselectivity

1. Introduction

Ethyl cellulose (EC) has been believed as a kind of polymer material with better membrane-forming ability, medium gas-separation/pervaporation capability, good flexibility, excellent durability, and low cost. From 1950 to the present, a few reports concerning the gas/vapor transport in the EC membrane appeared [1–12]. Weller and Steiner described the permeability of four gases through the EC membrane in a narrow temperature range [1]. Ito mentioned the permeability of four gases across the EC membrane [2]. Hsieh studied the permeability, solubility, and diffusivity of thirteen gases in the EC membrane [3]. Recently, Houde and Stern discussed the effect of ethoxy content on the permeability, solubility, and diffusivity of three light gases in EC membrane [4,5]. Suto et al. compared the oxygen (O_2)/nitrogen (N_2) permeability in EC membrane with and without liquid crystal order [6]. He et al. prepared a blend membrane of EC with oxygen carrier for the purpose of selective permeation of O_2 [7]. Wang and Easteal gave the results of O_2/N_2 transport in trifluoroacetylated EC membrane [8]. Very recently, Bai et al. fabricated a silver incorporated EC membrane for recovery of propylene from refinery off-gas mixture [9]. However, little report concerning a systematical investigation on the permeability, diffusivity, solubility, and their selectivities of O_2, N_2, carbon dioxide (CO_2), methane (CH_4), and hydrogen (H_2) through the EC membrane was found. Furthermore, the influence of temperature and upstream pressure on the permeability, diffusivity, solubility, and their selectivities of the gases through and in the EC membrane has not been well characterized, even though changes in operating temperature and pressure are known to affect significantly the performance of the EC membranes.

* Corresponding author. Address: Department of Polymer Materials Science and Engineering, College of Materials Science and Engineering, Tongji University, 1239 Siping Road, Shanghai 200092, People's Republic of China. Tel.: +86-21-65799455; fax: +86-21-65982461.

E-mail address: lixingui@citiz.net (X.-G. Li).

0032-3861/01/$ - see front matter © 2001 Published by Elsevier Science Ltd.
PII: S0032-3861(01)00121-5

The primary objective of our series of investigations is to elaborate the actual air-separation performance of EC-liquid crystal compound blend membranes [13–21]. In the present work, we attempt to provide a more complete understanding of gas transport in the free-standing EC membrane by investigating, over an unprecedented range of temperature and pressure, the permeability, diffusivity, and solubility of five gases through the membrane, and to elaborate the variation of its permeability, diffusivity, solubility, and their selectivities with temperature and pressure. A relationship between the diffusivity and effective molecule diameter of the gases across the EC membrane as well as between the gas solubility in the membrane and the critical temperature of the gases is discussed for the first time.

2. Experimental

2.1. Materials

EC particles produced by Shantou Xinning Chemical Works of Guangdong Province in China have the viscosity 0.04–0.08 Pa s measured in ethanol/toluene (1:1) at the concentration of 5 wt% at 25°C. The degree of substitution of the EC is ca. 2.4. The gases chosen for this study include O_2, N_2, CO_2, CH_4, and H_2. These gases were supplied by Messer Griesheim GmbH, Duesseldorf, Germany. The purity of CH_4 was higher than 99.5%, and the other gases had the purity of more than 99.99%. The EC, the gases, and chloroform of analytical reagent grade were directly used without any purification.

2.2. Membrane preparation

EC particles of 0.3 g were dissolved in 5 mL chloroform to form a 6 wt% solution. The polymer solution was poured into a Petri dish. Solvent was allowed to evaporate slowly from the solution at 25°C and 60% relative humidity for almost 20 h. The resultant membrane was removed from the Petri dish by pouring some water and dried in a high vacuum at 45°C for 4 h. EC membrane is flexible and transparent and has a thickness of 40 μm. This thickness, used for the calculation of permeability and diffusivity, was determined as a mean value from at least ten single measurements within the whole membrane area using a digital Mitutoyo gauge providing a resolution of 1 μm. The homogeneity of the membrane thickness is about 5%.

2.3. Morphology characterization

The EC membrane was characterized by wide-angle X-ray diffraction (WAXD) in a range of Bragg angle 2–40° using the wavelength 0.154 nm of CuKα electron beam in step-by-step scanning region and recorded nickel filtered radiation at 25°C with a Rigaku D/max-r A X-ray generator made in Japan. The scanning rate is 2°/min. Perkin–Elmer DSC 7 thermal analytical system was used to measure the glass transition temperature of the EC membrane at a heating rate of 10°C/min and a cooling rate of −10°C/min with a sample mass of 2.8 mg. The tensile property of a 9 mm-wide EC membrane was examined by an Instron Tensile Tester model 5565, made in USA.

2.4. Gas permeation measurements

The gas permeation performance of the EC membrane was measured using a constant volume, variable pressure approach by a standardized transient permeation technique with a self-built vacuum time-lag apparatus [22,23]. All parts are held at a constant temperature (±0.2°C) in an air bath inside a thermostatic housing. The effective permeation area was 7.07 cm^2. After both the sides of a membrane were evacuated, the pure gas was introduced to the upstream side of the membrane at a certain pressure, and was allowed to permeate to the downstream side at a pressure of 0.00001 bar. On the downstream side, a chamber of 43.8 cm^3 constant volume connected with a pressure gauge was attached to the membrane. After a certain period of time, a steady state was reached at which the amount of gas permeated increases linearly with time. The upstream and downstream pressures were measured by two pressure sensors and recorded online. The sensor can provide a resolution of 0.001 mbar corresponding to 0.01% of the full scale (10 mbar). The software developed in Technical University of Berlin ensures automated measurement with an automatically adapting data sampling rate to yield at least 600 data points and to describe time-lag and steady-state gas transport completely. For H_2, about 200 data point can be obtained before the permeate pressure reached 10 mbar. Feed pressure was adjusted from 1 to 20 bar. The permeate pressure was recorded up to 10 mbar, depending on the feed gas. It is found that the response time for the entire measuring system is shorter than 1 s. This was deemed adequate to provide high measuring accuracy. The permeability coefficient, P, was calculated from the slope of the straight line in the steady-state region by $P = J_S l/(p_2 - p_1)$ (J_S is the steady-state rate of gas permeation through a unit area of a membrane of thickness l, p_2 and p_1 are the upstream and downstream pressures of the gas component). These measurements were carried out at 25, 35, 45, and 55°C for oxygen, nitrogen, carbon dioxide, methane, and hydrogen. The apparent diffusion coefficient D was estimated from the time-lag τ by $D = l^2/(6\tau)$. The apparent solubility coefficient S was calculated from $S = P/D$. When the downstream pressure is negligible relative to the upstream pressure, the ideal separation factor of a membrane for a gas pair of A and B can be related simply to the ratio (P_A/P_B) of the permeabilities of A and B. Diffusion selectivity and solubility selectivity were defined as D_A/D_B and S_A/S_B, respectively. The experimental errors vary with the magnitudes of the permeability and time lag. The estimated errors in gas permeability, diffusivity, and solubility are about 3% for fast gases including O_2, CO_2, and H_2, and about 5% for

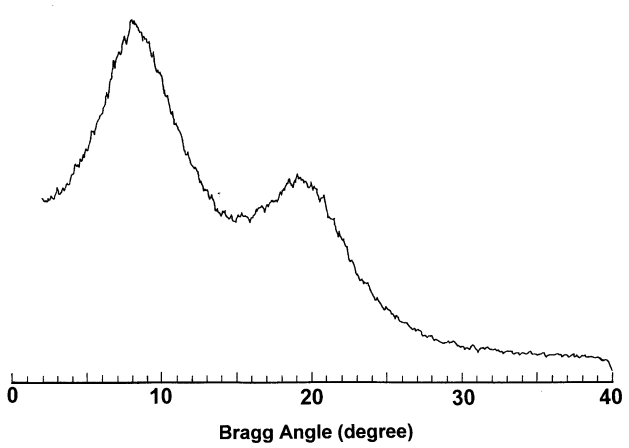

Fig. 1. Wide-angle X-ray diffraction diagram of the EC membrane.

slow gases such as N_2 and CH_4. The error might be larger at lower upstream pressures, especially for N_2 and CH_4 transport. The reproducibility is about 4% due to uncertainties of the determination of the downstream volume, the effective area and thickness of the membrane.

3. Results and discussion

3.1. Membrane characteristics

The EC membrane is smooth and flexible and looks homogeneous and transparent with a naked eye. A WAXD diagram of the EC membrane is shown in Fig. 1. Two major diffraction peaks at *d*-spacing of 1.11 nm (stronger) and 0.46 nm (weaker) are broad. A cooling differential scanning calorimetry (DSC) curve of the EC membrane is shown in Fig. 2. No crystallization exotherm is observed, implying that the no crystallization occurs during cooling. A very apparent endothermic break in the curve representing glass transition is observed. The linear portions of the curve just preceding and following the endothermic T_g break are extrapolated to their intersection as shown in Fig. 2. Glass transition temperature value is taken to be 80°C as the extrapolated endothermic break, because it was reported that this method has been shown to be reliable and reproducible [24].

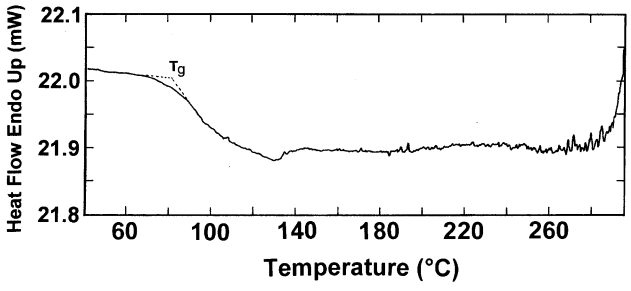

Fig. 2. Differential scanning calorimetry cooling thermogram of the EC membrane at a cooling rate of −10°C/min after a heating process (10°C/min) from room temperature to 300°C and maintain for 30 min at 300°C.

The difference of thermal capacity corresponding to the glass transition is 0.236 J/g K. The tensile stretching behavior of the EC film is shown in Fig. 3. There is an apparent yield point with the yield strength of 45 MPa and yield elongation of 11%. The tensile strength, initial modulus, and elongation at break of the membrane are determined to be 48 MPa, 560 MPa, and 28% respectively. All these results imply that the EC membrane is amorphous and can be served as a gas separation membrane with higher permeability, as discussed below. It is reported that EC cast membrane showed very little crystalline structure [3].

3.2. Gas permeation performance

Fig. 4 exhibits the variation of downstream pressure of five pure gases through the EC membrane with permeating time. Obviously, five gases permeate the membrane in different ways. H_2 can permeate the membrane very rapidly with a time-lag of shorter than 0.5 s because the molecular size of H_2 is small enough to pass freely through the free volume in the EC membrane due to a short-range motion of chain molecules such as the vibrational and/or rotational motions of side groups. CO_2 can also permeate the membrane very rapidly only after a long time-lag of 13 s. N_2 permeates the membrane most slowly, whereas CH_4 exhibits the second slowest permeation rate through the membrane after the longest time-lag of 22 s. It is because of the different permeation characteristics of various gases through the membrane that the EC membrane can be served as a high-performance membrane for gas separation. It should be noted that the EC dense membrane with the thickness of less than 40 μm can withstand high temperature (55°C) and very high pressure difference (20 bar) for a long period of time without any membrane destructure and permselectivity loss. This observed behavior may have practical utility when good performance stability is an issue.

3.3. Effect of temperature on gas permeability and its selectivity

CO_2 permeation through the EC membrane was recorded with increasing operating temperature from 298 to 328 K and is shown in Fig. 5. It can be seen that the downstream pressure of the membrane increases rapidly after a long initial time-lag. The increase rate of downstream pressure with permeating time is dependent on the temperature. The slope of straight line of downstream pressure versus permeating time in a steady-state region has been used to calculate the permeability. A typical relationship between gas permeability or permselectivity and reciprocal absolute temperature for EC membrane is shown in Fig. 6. The gas permeability through the membrane increased with an increase in temperature in a considered range of 25–55°C at a constant upstream pressure of 2 bar and is found to

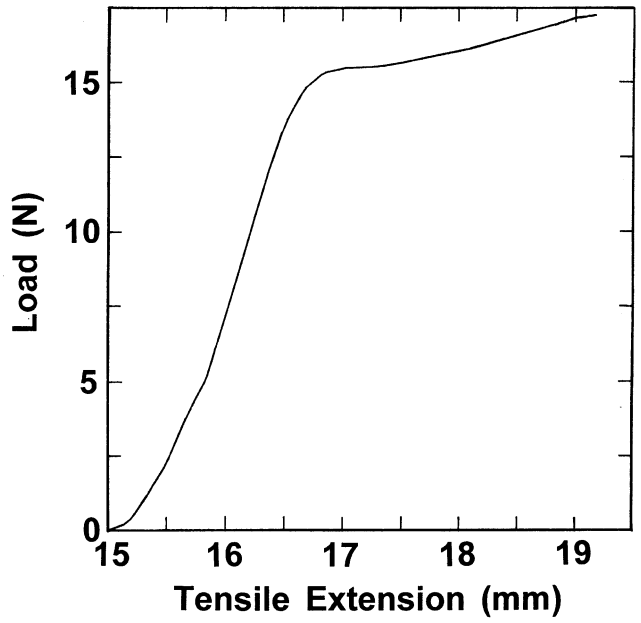

Fig. 3. Tensile stress–strain curve of EC membrane with the thickness of 0.04 mm and width of 9 mm at a stretching rate of 10 mm/min, relative humidity 77%, and 22°C.

follow the Arrhenius law,

$$P = P_0 \exp(-E_P/RT) \quad (1)$$

The activation energy (E_P) values for CO_2, O_2, H_2, N_2, and CH_4 permeation through the membrane calculated by the Arrhenius law are 3.3, 6.3, 6.9, 8.1, and 8.7 kJ/mol, respectively. It was reported that the permeation activation energy through other EC and other polymer membranes follows almost the same trend with a variation of permeation gas [1,22,23], that is, the E_P value for CO_2 is the smallest but the E_P value for CH_4 is the largest. Note that the permeation energy for the gases calculated in this paper is lower than

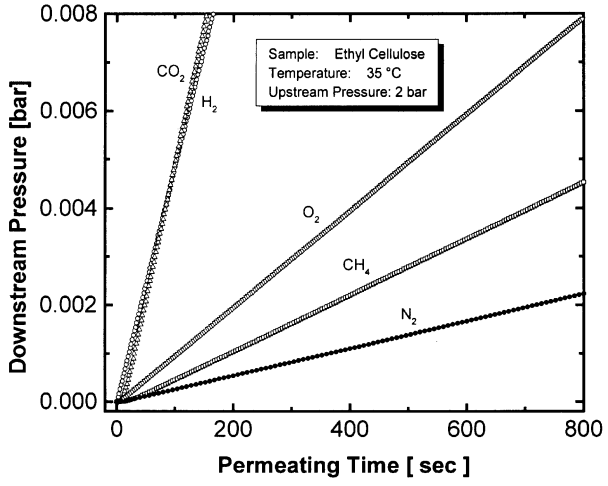

Fig. 4. Relationship between the downstream pressure and permeating time for the permeation of five gases through the ethyl cellulose (EC) membrane at an upstream pressures of 2 bar and 35°C.

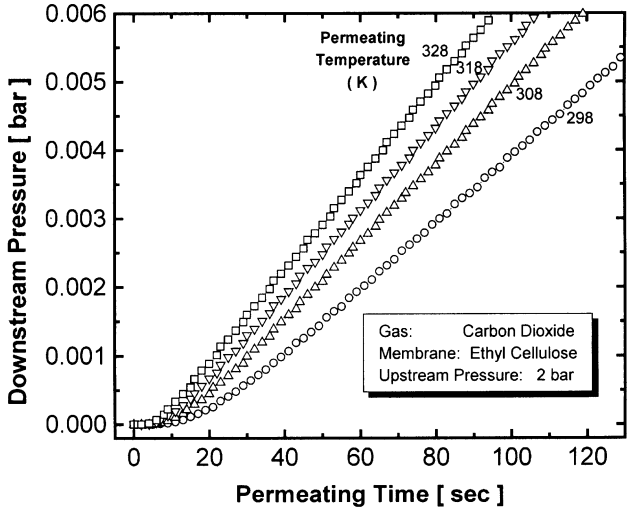

Fig. 5. Relationship between the downstream pressure and permeating time for carbon dioxide permeation through the ethyl cellulose (EC) membrane at an upstream pressure 2 bar and four permeating temperatures.

that in literature [2,6,7], possibly due to the differences in measurement conditions and the molecular structure of the ECs including their degree of substitution of ethyl group and molecular weight. Additionally, as shown in Fig. 6(b), there is a linear relation between the permselectivity of two gas pairs (O_2/N_2 and CO_2/CH_4) and reciprocal temperature. For the H_2/N_2, of the four points, three form an approximate straight line and the fourth is off. The permselectivity increases with enhancing reciprocal absolute temperature where P_{CO_2}/P_{CH_4} exhibits the strongest dependence on reciprocal temperature. This is a normal trend for most polymer membranes except for the liquid crystal membranes [13,15,16,18].

It can be seen from Fig. 6(a) that the permeability coefficients for the EC membrane at the temperature below 48°C increase in the order of gases

$$P_{N_2} < P_{CH_4} < P_{O_2} < P_{H_2} < P_{CO_2}$$

The lowest P_{N_2} is attributed to both the low diffusivity and the lowest solubility and the highest P_{CO_2} should be caused by its highest solubility of the five gases, as discussed below. A slightly different permeability order for the EC membrane at a temperature higher than 48°C is as follows:

$$P_{N_2} < P_{CH_4} < P_{O_2} < P_{CO_2} < P_{H_2}$$

The highest P_{H_2} should be due to its highest diffusivity at an elevated temperature regardless of its lowest solubility.

3.4. Effect of temperature on gas diffusivity and its selectivity

A typical relationship between gas diffusivity or its selectivity and reciprocal absolute temperature for EC membrane is shown in Fig. 7. The gas diffusivity through the

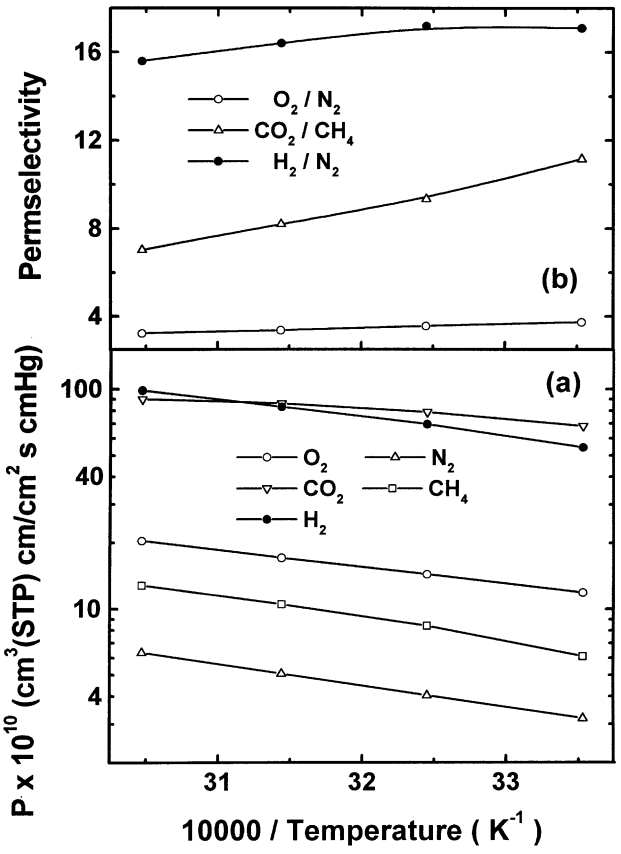

Fig. 6. The variation of permeability (a) and permeability selectivity (b) through the EC membrane with temperature at an upstream pressure of 2 bar.

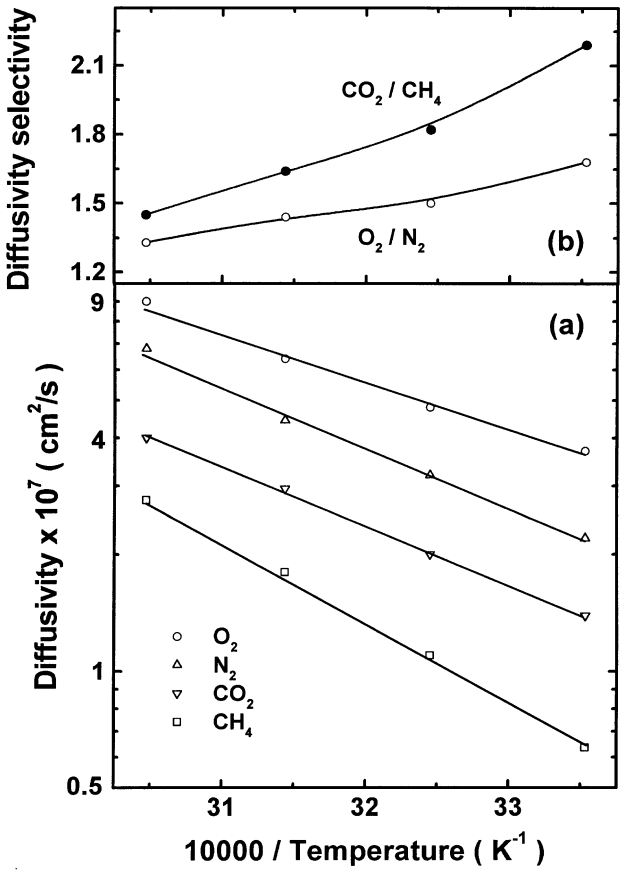

Fig. 7. The variation of diffusivity (a) and diffusivity selectivity (b) through the EC membrane with temperature at an upstream pressure of 2 bar.

membrane increased with an increase in temperature in a considered range of 25–55°C at a constant upstream pressure of 2 bar and is found to follow the Arrhenius law,

$$D = D_0 \exp(-E_D/RT) \quad (2)$$

The activation energy (E_D) values for the O_2, CO_2, N_2, and CH_4 diffusion through the membrane calculated by the Arrhenius law are 10.4, 12.6, 13.1, and 17.4 kJ/mol, respectively. It was reported that the diffusion activation energy through other polymer membranes follows almost the same trend with a variation in gas [23], that is, the E_D value for O_2 is the smallest but the E_D value for CH_4 is the largest. Additionally, as shown in Fig. 7(b), there is an apparently positive relation between the diffusivity selectivity and reciprocal temperature. The selectivity data exhibit an upward curvature. The diffusivity selectivity increases with enhancing reciprocal temperature where D_{CO_2}/D_{CH_4} exhibits stronger dependence on reciprocal temperature. This is a general trend for most polymer membranes.

It can be seen from Fig. 7 that the trend of the diffusion coefficients for four gases is quite different from the permeability coefficients as follows:

$$D_{CH_4} < D_{CO_2} < D_{N_2} < D_{O_2}$$

It should be noted that D_{O_2} is greater than those of other three gases through the membranes, since O_2 molecule has the smallest molecular diameter in the four gases. On the contrary, the smallest D_{CH_4} should be due to its largest molecular diameter. The second smallest D_{CO_2} through the membrane is attributed to the relatively high solubility and a nonspherical or linear molecular shape, especially the strong interaction of carbon dioxide with the membrane. The interaction hinders the mobility of CO_2 molecule through the membrane.

3.5. Effect of temperature on gas solubility and its selectivity

A typical relationship between gas solubility or its selectivity and reciprocal temperature for EC membrane is shown in Fig. 8. The gas solubility in the membrane increased with a decrease in temperature in a temperature range of 25–55°C at a constant upstream pressure of 2 bar and is found to follow the van't Hoff relationship,

$$S = S_0 \exp(-\Delta H_S/RT) \quad (3)$$

The solution heat (ΔH_S) values for O_2, N_2, CH_4, and CO_2

in the membrane calculated by the van't Hoff relationship are 4.4, 5.5, 8.8, and 9.9 kJ/mol, respectively. It was reported that the solution heat in other polymer membranes follows almost the same tendency of variation with a variation of solution gas [22], that is, the $-\Delta H_S$ value for CO_2 is the largest. Additionally, as shown in Fig. 8(b), there is an opposite linear relation between the solubility selectivity of two gas pairs and reciprocal temperature. The O_2/N_2 solubility selectivity increases but CO_2/CH_4 decreases with enhancing reciprocal temperature.

Fig. 8 also shows that the trend of the solubility coefficients for four gases is different from the trend of permeability and diffusivity.

$$S_{N_2} < S_{O_2} < S_{CH_4} < S_{CO_2}$$

The lowest S_{N_2} is due to its weakest interaction with the membrane. The greatest S_{CO_2} and CO_2/CH_4 solubility selectivity in the membrane is attributed to the relatively high solidification point and the strongest interaction of CO_2 with the membrane. It was reported that in an environment of stronger molecular interaction, the more condensable the gas is, the higher is the gas solubility [25].

The values of permeability, diffusivity, and solubility of various gases measured at 25°C and upstream pressure of 2 bar are summarized in Table 1. The highest permeability of a larger molecule such as CO_2 arises from its highest solubility, whereas the smallest molecule such as H_2 is the second most highly permeable because of its the highest diffusivity. The lowest permeability of N_2 is mainly attributed to its second lowest solubility. It can be seen that the gas permeability and diffusivity obtained in this study are lower than those reported in literature [2,3,6,7], whereas the solubility of O_2 and CO_2 obtained in this study is higher than literature value. The difference may arise from the difference in degree of substitution and molecular weight of EC, as well as membrane-forming and examining conditions. Table 2 summarizes the selectivity values of permeability, diffusivity, and solubility of three gas pairs at two temperatures. Apparently, higher permselectivity of O_2/N_2 and H_2/N_2 is mainly due to their larger diffusivity selectivity at 25°C, whereas higher permselectivity of CO_2/CH_4 is mainly due to its larger solubility selectivity. When the temperature is elevated to 55°C, the gas permselectivity of three gas pairs decreases because their diffusivity selectivity decreases significantly regardless of an increase in solubility selectivity of O_2/N_2 and H_2/N_2.

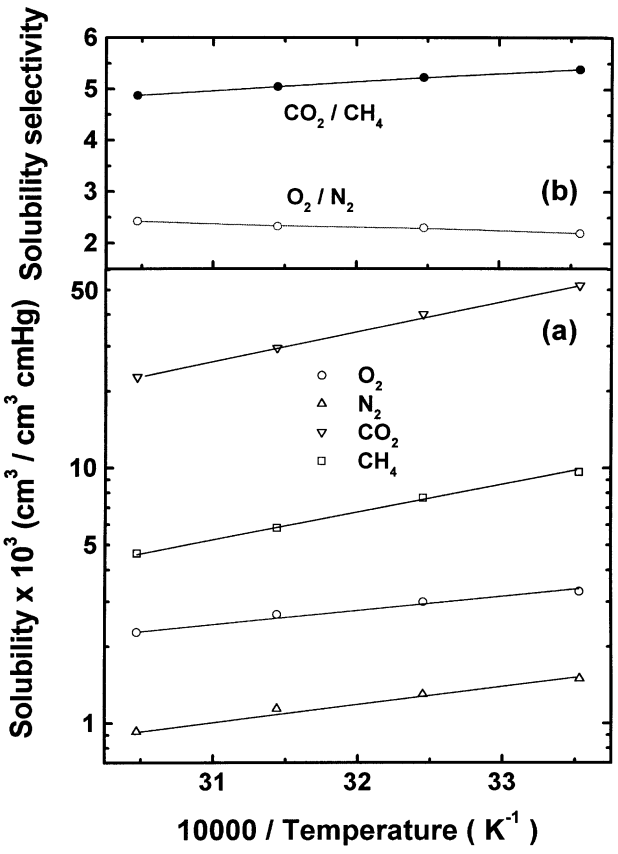

Fig. 8. The variation of solubility (a) and solubility selectivity (b) in the EC membrane with temperature at an upstream pressure of 2 bar.

Table 1
Effective molecular diameter (σ_{eff}) and critical temperature (T_c) of gases and their permeability (P), diffusivity (D), and solubility (S) across EC membrane at 25°C and 2 bar

Gas	H_2	O_2	CO_2	N_2	CH_4
σ_{eff} (nm)	0.290	0.344	0.363	0.366	0.381
T_C (°C)	33.3	154.4	304.2	126.2	190.7
Permeability[a]	54.4(86.8)[b]	11.9(14.6)[c]	67.7(112.8)[c]	3.18(4.4)[c]	6.10
Diffusivity[d]	490	40.1(63.9)[c]	14.1(56.5)[c]	20.0(23.3)[c]	6.35
Solubility[e]	1.11	2.97(2.3)[c]	48.0(20)[c]	1.59(1.9)[c]	9.61

[a] The unit of permeability is 10^{-10} cm^3(STP) cm/cm^2 s cmHg.
[b] The datum in the parentheses is obtained at 20°C from Ref. [2].
[c] The data in the parentheses are obtained from Ref. [3].
[d] The unit of diffusivity is 10^{-8} cm^2/s.
[e] The unit of solubility is 10^{-3} cm^3(STP)/cm^3 cmHg.

Table 2
Selectivity of permeability, diffusivity, and solubility of gases across EC membrane at an upstream pressure of 2 bar

Selectivity	25°C			55°C		
	O_2/N_2	CO_2/CH_4	H_2/N_2	O_2/N_2	CO_2/CH_4	H_2/N_2
Permeability	3.74(3.32)[a]	11.1	17.1	3.23	6.97	15.7
Diffusivity	2.01(2.74)[a]	2.22	24.5	1.39	1.45	7.28
Solubility	1.86(1.21)[a]	5.00	0.68	2.33	4.81	2.15

[a] The data in the parentheses are calculated on the basis of the permeability from Ref. [3].

3.6. Effect of upstream pressure on gas permeability and its selectivity

The O_2 permeation through the EC membrane was recorded with increasing upstream pressure from 2 to 20 bar and is shown in Fig. 9. It can be seen that the downstream pressure of the membrane increases rapidly after a small initial time-lag. The increase rate of downstream pressure with permeating time is strongly dependent on the upstream pressure. The slope of straight line of downstream pressure versus permeating time in a steady-state region has been used to calculate the permeability. The permeability of five gases through the EC membrane at 25°C is shown in Fig. 10 as a function of upstream pressure from 2 to 20 bar. The permeability of O_2, N_2, and CH_4 does not appear to be affected by pressure up to 20 bar [26], while CO_2 and H_2 permeabilities seem to increase slightly. It should be noted that P_{CO_2} and P_{H_2} slightly increased with increasing pressure, leading to an increase in P_{CO_2}/P_{CH_4} and P_{H_2}/P_{N_2} in the corresponding pressure range. Slightly positive P_{CO_2} and P_{H_2} dependence on upstream pressure could be because the pore blocking effect for hydrogen with the smallest molecular size among the five gases does not play such a significant role as the other four gases. A similar P_{CO_2}

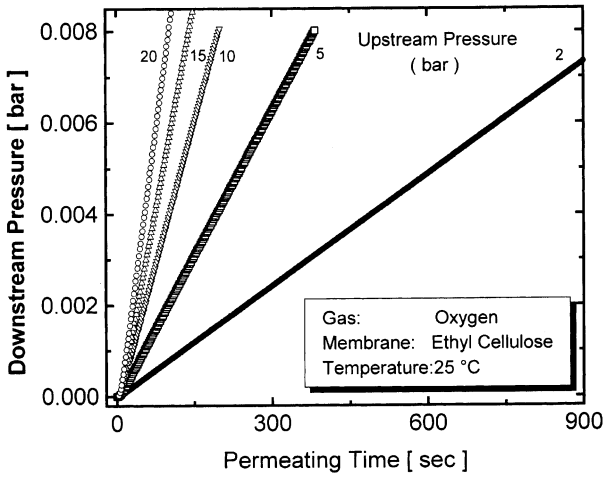

Fig. 9. Relationship between the downstream pressure and permeating time for oxygen permeation through the ethyl cellulose (EC) membrane at different upstream pressures and 25°C.

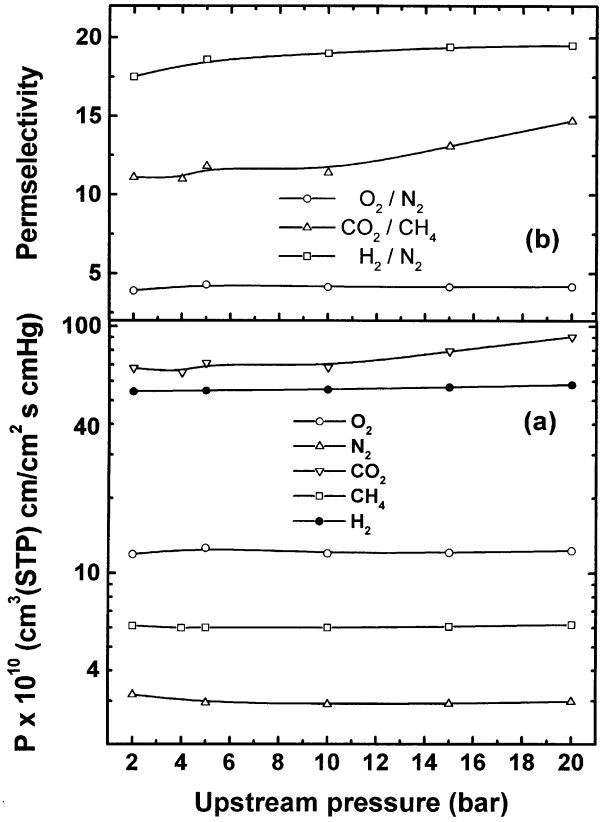

Fig. 10. The variation of permeability (a) and permeability selectivity (b) through the EC membrane with upstream pressure at 25°C.

or P_{He} versus upstream pressure relationship has been reported for a rubbery polydimethylsiloxane membrane [27] and glassy 4-vinylpyridine-grafted polymethylpentene membrane [28]. This is beneficial to the practical CO_2/CH_4 and H_2/N_2 separation because P_{CO_2}, P_{H_2}, P_{CO_2}/P_{CH_4}, and P_{H_2}/P_{N_2} can be increased concurrently with increasing upstream pressure.

3.7. Effect of upstream pressure on gas diffusivity and its selectivity

The diffusivity of four gases through the EC membrane at 25°C is shown in Fig. 11 as a function of upstream pressure from 2 to 20 bar. The diffusivity of O_2 and N_2 with smaller molecular diameter through the EC membrane decreases but the diffusivity of CO_2 and CH_4 with larger molecular diameter increases slightly with increasing upstream pressure, leading to almost constant D_{O_2}/D_{N_2} and D_{CO_2}/D_{CH_4} values in the corresponding pressure range. The positive pressure-dependent diffusivity has been interpreted by using a partial immobilization model [28]. It is of interest that the D_{CO_2} value exceeds D_{N_2} value in an elevated pressure region, which should be attributed to the plasticization effect owing to the higher sorption capability of CO_2 in the membrane. A similar result has been observed for the polyvinylpyridine membrane [25].

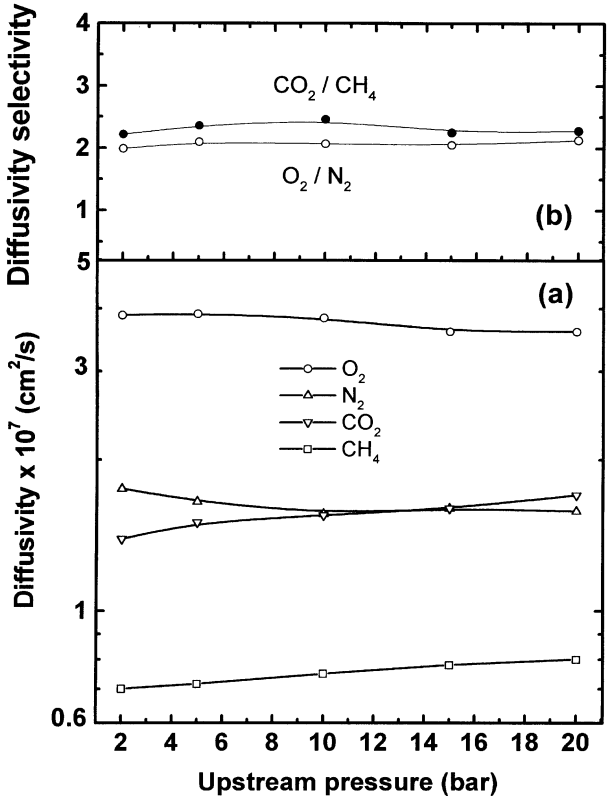

Fig. 11. The variation of diffusivity (a) and diffusivity selectivity (b) through the EC membrane with upstream pressure at 25°C.

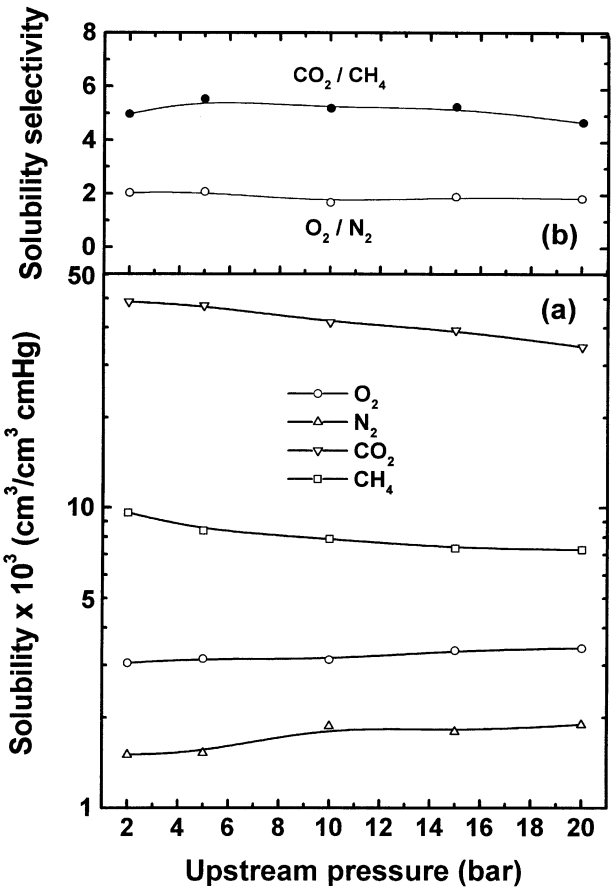

Fig. 12. The variation of solubility (a) and solubility selectivity (b) in the EC membrane with upstream pressure at 25°C.

3.8. Effect of upstream pressure on gas solubility and its selectivity

The diffusivity of four gases through the EC membrane at 25°C is shown in Fig. 12 as a function of upstream pressure from 2 to 20 bar. The solubility of O_2 and N_2 with lower critical temperature in the EC membrane increases but the solubility of CO_2 and CH_4 with higher critical temperature decreases slightly with increasing upstream pressure, leading to almost constant S_{O_2}/S_{N_2} and S_{CO_2}/S_{CH_4} values in the corresponding pressure range. The negative pressure-dependent solubility has been interpreted by using a partial immobilization model [25].

3.9. Relationship between gas diffusivity and molecular diameter

Fig. 13 gives plots of the gas diffusivity versus square value of effective molecular diameters at different temperatures or upstream pressures on the basis of the empirical relationship between gas diffusivity and effective diameter (σ_{eff}) of gas molecules listed in Table 1 by the following Eq. (4)

$$D = K_1 \exp\left[-K_2(\sigma_{\text{eff}})^2\right] \tag{4}$$

where K_1 and K_2 are constants and

$$(\sigma_{\text{eff}})^2 = (\text{collision diameter} \times \text{kinetic diameter}) \tag{5}$$

Three straight lines with different slopes are obtained, as shown in Fig. 13(a). It appears that a smaller slope is observed at the higher temperature or higher upstream pressure. That is to say, the dependence of gas diffusivity on the effective molecular diameter becomes weaker with increasing temperature or upstream pressure. Note that only CO_2 and N_2 data points deviate from the straight lines sometimes. A very similar result has been obtained for polyvinylpyridine membrane [25]. It was reported that the diffusion process of the gas penetrant occurs along a cylindrical volume defined by the penetrant diameter, σ_{eff}, and the average length of its diffusional step, λ. The product of the cylindrical volume and the cohesive energy density, E_{coh}, of the polymer equals the activation energy for diffusion as follows [29]:

$$E_{\text{D}} = (\pi/4)\sigma_{\text{eff}}^2 \lambda E_{\text{coh}} \tag{6}$$

On the basis of Eq. (6), Fig. 13(b) shows a reasonable relationship between E_{D} values and the square of the effective diameter (σ_{eff}) of gases. If the effective diameter,

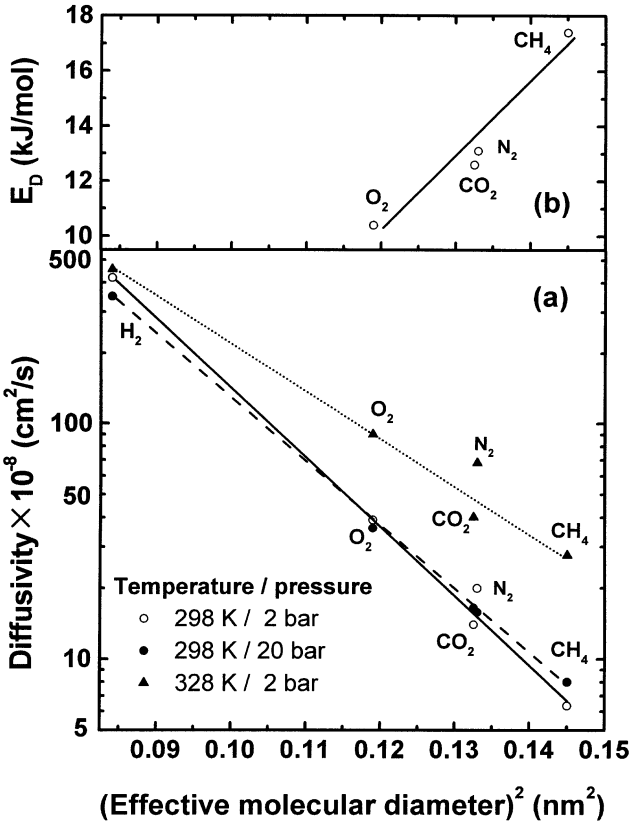

Fig. 13. (a) Gas diffusivity across the EC membrane as a function of the square of effective gas molecule diameter at two temperatures and two upstream pressures. (b) Correlation of activation energy for diffusion with gaseous penetrant sizes across EC membrane.

σ_{eff}, is replaced with kinetic diameter, the linearity of the relationship will be poorer. Note that the E_D values for CO_2 and N_2 appear to be lower. H_2 is not included in this plot since its activation energy of diffusion was not obtained due to difficulty in measuring H_2 diffusivity at several temperatures with precision. Similar relation between E_D values and the square of the molecular diameter of gases through tetramethyl polycarbonate was reported [29].

3.10. Relationship between gas solubility and critical temperature (T_C)

The gas solubility in the membrane is correlated with critical temperature (T_C) listed in Table 1 by Eq. (7)

$$\ln S = \ln S_0 + K_C T_C \quad (7)$$

where S_0 and K_C are constants. The critical temperature is a measure of the ease of condensation for gaseous molecules. The solubility of five gases in the EC membrane as a function of critical temperature is shown in Fig. 14. It is seen that the solubility increases almost linearly as the critical temperature increases. Only the H_2 data point deviates significantly from the straight line. A similar relationship

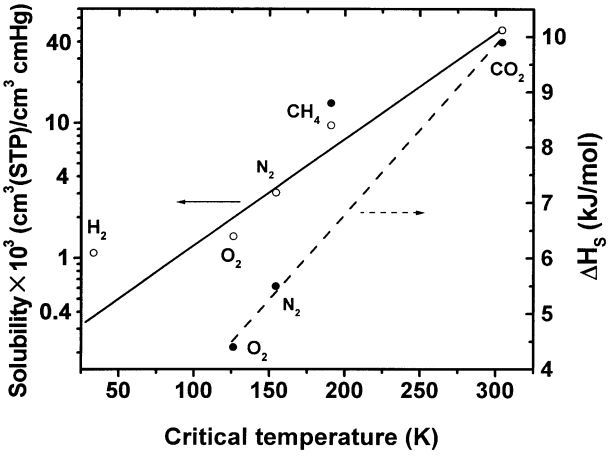

Fig. 14. Gas solubility and solution heat in the EC membrane as a function of critical temperature at an upstream pressure of 2 bar and 25°C.

between solubility and critical temperature of the gases was also observed for polyvinylpyridine [25]. In addition, the solution heat seems to be well correlated with critical temperature of gases, as shown in Fig. 14. Only the solution heat for CH_4 deviates significantly from the straight line, possibly due to the difference in the interaction of CH_4 with EC as compared with other three gases. Almost the same correlation of solution heat with the critical temperature of gases in tetramethyl polycarbonate has been observed [29].

4. Conclusions

The temperature dependence of permeability, diffusivity and solubility through and in the EC membrane acts in accordance with the Arrhenius equation and a van't Hoff relationship, respectively. The activation energy E_P of gas permeation is primarily governed by changes in diffusion activation energy since $|E_D| > |\Delta H_S|$ for each gas. Different upstream pressure-dependent behaviors for the permeation, diffusion, and solution of gases through and in the EC membrane have been found. The size of gas molecules affects significantly the diffusion performance across the membrane. A linear relationship between effective molecule diameter of the gases and their diffusivity/diffusion activation energy through the EC membrane has been found. There is an almost linear relationship between the critical temperature and solubility/solution heat of the gases in the EC membrane.

Acknowledgements

The project was supported by (1) the National Natural Science Fund of China (29804008); (2) the Fund of the University Key Teacher by Chinese Ministry of Education (GG-430-10247-1186); (3) the Phosphor Plan of Science

Technology for Young Scientists of Shanghai China (98QE14027); (4) the State Key Laboratory for Modification of Chemical Fibers and Polymer Materials at Donghua University, Shanghai, China; (5) the Fund of Visiting Professor of Technical University of Berlin, Germany.

References

[1] Weller S, Steiner WA. J Appl Phys 1950;21:279.
[2] Ito Y. Kobunshi Kagaku 1961;18:124.
[3] Hsieh PY. J Appl Polym Sci 1963;7:1743.
[4] Houde AY, Stern SA. J Membr Sci 1994;92:95.
[5] Houde AY, Stern SA. J Membr Sci 1997;127:171.
[6] Suto S, Niimi T, Sugiura T. J Appl Polym Sci 1996;61:1621.
[7] He Y, Yang J, Li H, Huang P. Polymer 1998;39:3393.
[8] Wang Y, Easteal AJ. J Membr Sci 1999;157:53.
[9] Bai S, Sridhar S, Khan AA. J Membr Sci 2000;174:67.
[10] Barrer RM, Barrie JA, Slater J. J Polym Sci 1957;23:315.
[11] Barrer RM, Barrie JA, Slater J. J Polym Sci 1958;27:177.
[12] Ravindra R, Sridhar S, Khan AA, Rao AK. Polymer 2000;41:2795.
[13] Li X-G, Huang M-R, Lin G, Yang P-C. J Appl Polym Sci 1994;51:743.
[14] Huang M-R, Li X-G, Lin G. Sep Sci Technol 1995;30:449.
[15] Li X-G, Huang M-R. Angew Makromol Chem 1994;220:151.
[16] Li X-G, Huang M-R, Lin G, Yang P-C. Colloid Polym Sci 1995;273:772.
[17] Li X-G, Huang M-R, Lin G. J Membr Sci 1996;116:143.
[18] Huang M-R, Li X-G. Gas Sep Purification 1995;9:87.
[19] Li X-G, Huang M-R. J Appl Polym Sci 1997;66:2139.
[20] Li X-G, Huang M-R, Hu L, Lin G, Yang P-C. Eur Polym J 1999;35:157.
[21] Li X-G, Huang M-R, Gu G-F, Qiu W, Lu J-Y. J Appl Polym Sci 2000;75:458.
[22] Kresse I, Usenko A, Springer J, Privalko V. J Polym Sci Part B 1999;37:2183.
[23] Xu ZK, Boehning M, Springer J, Steinhauser N, Muelhaupt R. Polymer 1997;38:581.
[24] Cassidy PE. Thermally Stable Polymers. New York: Marcel Dekker, 1980. p. 18.
[25] Shieh J-J, Chung TS. J Polym Sci Part B 1999;37:2851.
[26] Li X-G, Kresse I, Springer J, Nissen J, Yang Y-L. Polymer 2001;42:6849.
[27] Yeom CK, Lee SH, Lee JM. J Appl Polym Sci 2000;78:179.
[28] Lai JY, Wei SL. J Appl Polym Sci 1986;32:5763.
[29] Costello LM, Koros WJ. J Polym Sci Part B 1994;32:701.